Continuum angular distributions in preequilibrium nuclear reactions: Physical basis for Kalbach systematics

M.B. Chadwick[1] and P. Obložinský[2]

[1] *University of California, Nuclear Data Group, Lawrence Livermore National Laboratory, Livermore, California 94550*

[2] *Nuclear Data Section, International Atomic Energy Agency, 1400 Vienna, Austria*

(Received 22 June 1994)

We show how momentum conservation is fundamental to the description of angular distributions in preequilibrium nuclear reactions. By using state densities with linear momentum to describe the phase space during the preequilibrium cascade, angular distributions can be derived in a transparent way. Fermi-motion and Pauli-blocking effects are included, and correlations between the emission particle's energy and angle are obtained for all orders of scattering. Our model provides a physical basis for many features of the widely used phenomenological systematics of Kalbach, and provides a framework for understanding the systematical properties of continuum angular distributions.

PACS number(s): 24.60.Gv, 24.60.Dr, 25.40.Fq, 24.50.+g

Particles ejected during the early stages of a nuclear reaction are typically of high energy and have forward-peaked angular distributions, since they are emitted prior to nuclear equilibration and partially preserve the incident projectile's direction of motion [1–7]. These pre-equilibrium particles account for the continuum region of double differential emission spectra. Theoretical attempts to understand such spectra span from semiclassical approaches, notably exciton and hybrid models, up to recent quantum mechanical multistep theories [8]. The quantum mechanical approaches have been used with a certain amount of success for analyzing nucleon reactions up to 200 MeV. However, they still face open questions regarding the formulation of multistep processes [9], multiple particle emission, and the emission of complex particles. Semiclassical models have provided a clear insight into the physics of preequilibrium processes and have successfully explained many angle-integrated spectra, though they were initially not formulated to account for angular effects. Therefore a widely adopted approach [1–4] is to use these angle-integrated spectra, and obtain angular distributions from the Kikuchi-Kawai [10] nucleon-nucleon scattering kernel in a Fermi gas. While this has been able to explain certain features of the forward peaking, it has not been able to account for many of the systematic properties of continuum angular distributions [11]. Furthermore, most works assume a fast leading particle that carries all the directional information during the cascade. This is in contradiction to the equiprobability assumption used in the exciton model which puts all the excited particles and holes on an equal footing, and does not follow the individual particle's motion [2].

In the absence of a sufficient theoretical understanding of the general properties of continuum angular distributions, Kalbach developed phenomenological systematics to describe them [11]. She analyzed a large body of experimental measurements (over 900 data sets) in nucleon and alpha-induced reactions at energies up to several hundreds of MeV, and found simple angular variations and a surprising similarity between angular distributions in reactions involving varying types of projectile and ejectile. While these systematics are very useful for describing and predicting differential cross sections, their physical basis has remained obscure. The fact that observed continuum preequilibrium cross sections tend to vary smoothly with angle and energy, and lend themselves to simple parametrizations [11], suggests that they should be describable using a relatively simple model of the reaction process. In this paper we show how momentum considerations are fundamental to the description of continuum angular distributions, and using a semiclassical preequilibrium model we derive Kalbach's parametrization of the forward-peaking shape.

Our derivation applies to reactions involving both nucleons and complex particles, and relies on the use of state densities with linear momentum, which we introduced in Refs. [6, 7]. These densities describe the linear momentum structure of the phase space of excited particles and holes (excitons), and are closely related to angular-momentum-dependent state densities [7]. In the exciton model the emission rate from the nth preequilibrium stage containing p particles and h holes ($n = p+h$), leaving p_r particles and h_r holes in the residual nucleus, is obtained by applying detailed balance. By explicitly conserving linear momentum we obtain an angle-dependent rate for emission with energy ϵ and direction Ω given by

$$\frac{d^2\lambda_n(\epsilon,\Omega)}{d\epsilon d\Omega} = \frac{2\mu\epsilon\sigma_{\rm inv}}{\pi^2\hbar^3}\frac{\rho(p_r,h_r,E-\epsilon_\Omega,\mathbf{K}-\mathbf{k}_\Omega)}{4\pi\ \rho(p,h,E,\mathbf{K})}, \qquad (1)$$

where for clarity we have omitted model-dependent factors which may be applied to account for the type of ejectile particle [8]. μ is the ejectile reduced mass, and the reaction cross section for the inverse process is $\sigma_{\rm inv}$. The composite system total energy and momentum before particle emission are E and $\mathbf{K}$, respectively, and the residual nucleus energy and momentum after emission are $E-\epsilon_\Omega$ and $\mathbf{K}-\mathbf{k}_\Omega$, respectively, all these quantities being measured relative to the bottom of the nuclear well. The

energy and momentum of the emitted particle relative to the bottom of the nuclear well are $\epsilon_\Omega = \epsilon + B_{\rm em} + \epsilon_F$ and $\mathbf{k}_\Omega$, where $|\mathbf{k}_\Omega| = \sqrt{(2\mu\epsilon_\Omega)}$, $B_{\rm em}$ being the emission particle separation energy and ϵ_F the Fermi energy. Momentum, like energy, is not transferred to the whole residual nucleus; rather, it is carried solely by the excited particles and holes. The forward-peaked angular variation for a given emission energy follows directly from the variation of $\rho(p_r, h_r, E - \epsilon_\Omega, \mathbf{K} - \mathbf{k}_\Omega)$ with angle Ω in Eq. (1). This in turn follows from the inclusion of Fermi-motion and Pauli-blocking in the state densities, and ignores deviations from center-of-mass isotropy in nucleon-nucleon scattering. During the preequilibrium cascade our model assumes that particle-hole states can be populated providing that both energy and momentum are conserved, and the memory of the initial projectile direction is not maintained solely by a fast leading particle, but rather it is carried by both the excited particles and the holes.

The state density with linear momentum can be expressed [7] as the product of a state density in energy space, $\rho(p, h, E)$, and a linear momentum distribution function $M(p, h, E, \mathbf{K})$,

$$\rho(p, h, E, \mathbf{K}) = \rho(p, h, E)\ M(p, h, E, \mathbf{K}), \tag{2}$$

in analogy to the usual partitioning of the angular momentum state density. It has units of $\mathrm{MeV}^{-1}(\mathrm{MeV}/c)^{-3}$, is independent of the direction of $\mathbf{K}$, and yields the energy-dependent state density when integrated over all momenta, $\int \rho(p, h, E, \mathbf{K}) 4\pi K^2 dK = \rho(p, h, E)$. The individual momenta of the particles and holes are oriented in random directions, and the state density with linear momentum counts all configurations which sum to the required total energy and total momentum. The central limit theorem implies that the ensemble of the various particle and hole momenta sum to yield a distribution of total momenta which follows a Gaussian,

$$M(p, h, E, \mathbf{K}) = \frac{1}{(2\pi)^{3/2}\sigma^3} \exp(-K^2/2\sigma^2), \tag{3}$$

where σ is the momentum cutoff (representing the width of the distribution). This Gaussian solution has been shown to accurately describe the momentum distribution even when the number of excitons is small [7]. The momentum cutoff can be obtained by considering the average-squared value of the exciton momentum projections on the direction of $\mathbf{K}$ in a Fermi-gas nucleus, giving

$$\sigma^2 = n \left(\frac{2m\epsilon_{\rm av}}{3}\right), \tag{4}$$

where m is the nucleon mass, and $\epsilon_{\rm av}$ is the average exciton energy relative to the bottom of the nuclear well. Thus, as n increases with more excited particles and holes, the width of the total momentum distribution increases. If the excitation energy is less than the Fermi energy and $p \approx h$, then $\epsilon_{\rm av} \approx \epsilon_F$, but in general in an equidistant single-particle model it is given by

$$\epsilon_{\rm av} = \frac{2p(p+1)}{ng} \frac{\rho(p+1, h, \tilde{E})}{\rho(p, h, \tilde{E})} - \frac{\tilde{E}}{n} + \epsilon_F, \tag{5}$$

with the notation that $\tilde{E}$ denotes the excitation energy relative to the Fermi level, $\tilde{E} = E - (p - h)\epsilon_F$, and the state densities in Eq. (5) are taken from the equidistant model with finite well-depth restrictions [12].

Following the preequilibrium emission of a particle with momentum $\mathbf{k}_\Omega$, the squared absolute value of the residual nucleus momentum is

$$|\mathbf{K} - \mathbf{k}_\Omega|^2 = K^2 + k_\Omega^2 - 2Kk_\Omega \cos\theta,$$

where θ is the angle of emission in relation to the projectile direction. This residual-nucleus momentum appears in the state density in the numerator of Eq. (1) and accounts for the angular-dependence of the emission rate. Since the cross section for emission is proportional to the emission rate, we obtain

$$\frac{d^2\sigma_n(\epsilon, \Omega)}{d\epsilon d\Omega} = \frac{d\sigma_n(\epsilon)}{d\epsilon} \frac{1}{4\pi} \frac{2a_n}{e^{a_n} - e^{-a_n}} \exp(a_n \cos\theta), \tag{6}$$

where $d\sigma_n(\epsilon)/d\epsilon$ is the nth-stage angle-integrated exciton model cross section, the preexponential factor arises from the normalization conditions, and

$$a_n = \frac{3Kk_\Omega}{2n_r m\epsilon_{\rm av}}, \tag{7}$$

where $n_r = p_r + h_r$. The total preequilibrium emission is a sum of the above contributions for all preequilibrium stages. Conservation of linear momentum, and hence angle-energy correlation, is maintained for all orders of scattering. As would be expected, the forward peaking increases with incident and emission energy, and decreases with increasing n as the incident momentum is shared among more particles and holes.

Equation (6) has exactly the same functional form that Kalbach used to describe the preequilibrium angular distributions. In our derivation the angular variation as an exponential in $\cos\theta$ results from the Gaussian accessible phase space, and the vector addition of momenta using the cosine formula. Our model therefore explains the general shape of measured continuum angular distributions [11] and its applicability to various projectile and ejectile types. It also explains the observed independence of target mass. While the Kalbach-systematics formula is of the same functional form as our result, her expression applies to the full preequilibrium spectrum whereas ours applies to each preequilibrium stage component. The variable "a" that she parametrized by comparisons with many measurements can be understood as an averaged value of our a_n over all preequilibrium stages.

Our model also provides a framework for understanding other previously unexplained features of the systematic behavior of angular distributions: (1) Why the approximate independence of Kalbach's a parameter on incident energy below 130 MeV? This would arise by the approximate canceling of the incident energy dependence in our expression for a_n with the increasing number of preequilibrium stages (each with successively flatter angular distributions) that contribute. (2) Why the approximate independence on projectile mass in nucleon-emission reactions? In our approach, a_n increases as the

projectile mass increases, but this is (partly, at least) compensated by the increased number of excitons n in the preequilibrium cascade for complex-particle induced reactions. Once the mechanism for reactions involving complex particles has been established, the number of excitons in the residual nucleus can be determined and the angular distributions obtained.

There are similarities between our model and exciton models which use the Kikuchi-Kawai angular kernel. If instead of using our Gaussian (statistical) solution, the state densities with linear momentum are determined in a Fermi gas by convoluting single-particle densities while conserving energy and momentum, the Kikuchi-Kawai result follows for 1-step scattering [7]. But our result for multistep scattering differs from a convolution of Kikuchi-Kawai kernels since we do not make a leading-particle assumption. We showed in Ref. [7] that the Gaussian solution approximates the exact Fermi-gas result very well even when the number of excitons is small. We are further encouraged to use the Gaussian solution since Reffo and Herman [13] found that a Gaussian angular momentum distribution described shell-model with BCS pairing calculations well, even when there are just two excitons.

We compare angular distributions predicted by our linear-momentum conserving exciton model with a sample of experimental measurements for nucleon reactions, where the reaction mechanism is well established. Even though our model includes the quantum phenomena of Fermi motion and Pauli blocking, it does not account for other quantum effects such as refraction and diffraction from the nuclear potential, and finite-size effects. At low incident energies these have been shown to be important for obtaining sufficient backward-angle emission [2–4, 14], and result in a flatter angular distribution. A simple applications-oriented way to account for these effects is to modify a_n in Eq. (7) so that it is decreased by an energy-dependent parameter ζ. Writing a_n in terms of channel energies we then obtain for nucleon reactions

$$a_n = \frac{3\sqrt{(\epsilon_{\rm in} + B_{\rm in} + \epsilon_F)(\epsilon + B_{\rm em} + \epsilon_F)}}{\zeta\ (n-1)\epsilon_{\rm av}}, \qquad (8)$$

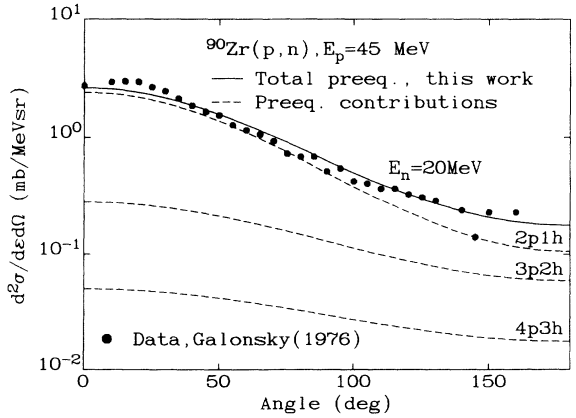

FIG. 1. Calculated angular distribution of 20 MeV neutrons in the 45 MeV ^{90}Zr(p,n) reaction compared with experimental data [16]. Contributions from different preequilibrium stages are shown, $2p1h$ being the initial stage.

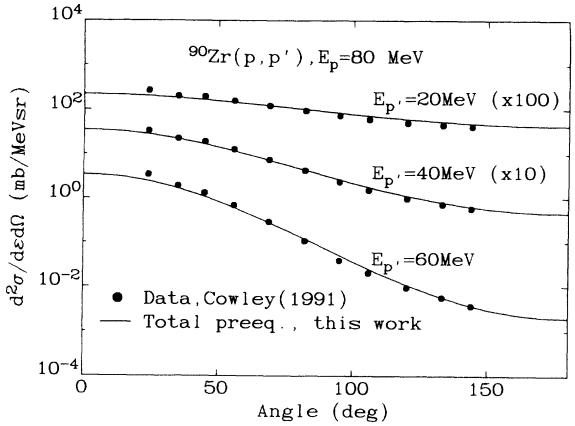

FIG. 2. Calculated angular distributions in the 80 MeV ^{90}Zr(p,p') reaction compared with experimental data [17].

and we take the Fermi energy as 35 MeV. By analyzing a few experimental data sets we have found that the simple parametrization $\zeta = \max(1, 9.3/\sqrt{\epsilon})$, with ϵ in MeV, works fairly well up to 80 MeV. This factor tends to 1 for the higher emission energies where the quantum effects become small, and increases to 2 at 20 MeV. Above 80 MeV, contributions from multiple preequilibrium processes can be significant, and while our model can be generalized to describe such processes, a more involved treatment is needed. It can also be straightforwardly extended to include a distinguishing of neutron and proton excitations in a two-component formalism.

We calculate exciton model cross sections using the GNASH [15] code and analyze three different preequilibrium reactions which span a range of energies and nucleon projectile and ejectile types. In Fig. 1 we show calculated angular distributions compared with experimental data of Galonsky *et al.* [16], for the 45-MeV induced ^{90}Zr(p,n) reaction. Contributions from various preequilibrium stages are indicated for a 20 MeV emission energy. The forward peaking is seen to decrease for higher-stage preequilibrium emission. Our model is compared with the 80-MeV induced ^{90}Zr(p,p') reaction measured by Cowley *et al.* [17] in Fig. 2 and the 26-MeV

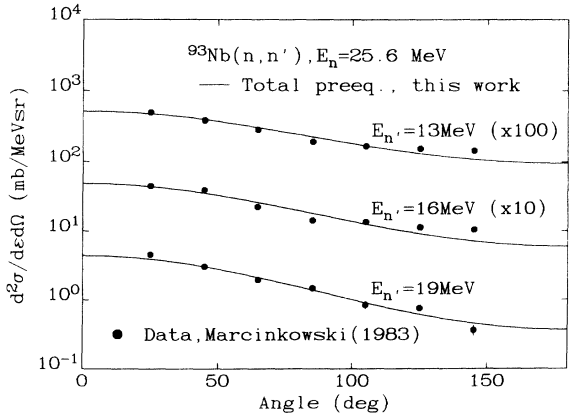

FIG. 3. Calculated angular distributions in the 26 MeV ^{93}Nb(n,n') reaction compared with experimental data [18].

induced ^{93}Nb(n,n') reaction measured by Marcinkowski *et al.* [18] in Fig. 3, and is seen to account for the experimental data well.

In summary, our model accounts for many features of observed continuum angular distribution: the angular shape as an exponential in cos θ that is seen for all projectile/ejectile types up to several hundreds of MeV; the target-mass independence; and we give a theoretical prediction for the a parameter which governs the degree of forward peaking. Use of state densities with linear momentum enables these distributions to be obtained using simple (and exact) expressions, and describes the decrease in forward peaking with increasing number of scatterings. The model is straightforward to apply computationally since the usual exciton model can be used for the angle-integrated cross section, and describes measurements well when modifications that approximate quantum finite-size and refraction effects are included. We have shown how momentum conservation is fundamental to the description of angular distributions in preequilibrium nuclear reactions. This observation may be of broader interest to other phenomena involving the evolution of quantal systems towards equilibrium.

We gratefully acknowledge useful discussions with M. Blann, C. Kalbach-Walker, and A. Kerman. This work was performed under the auspices of the U.S. Department of Energy by Lawrence Livermore National Laboratory under Contract No. W-7405-Eng-48.

[1] Sun Ziyang, Wang Shunuan, Zhang Jingshang, and Zhou Yizhong, Z. Phys. A **305**, 61 (1982).
[2] C. Costa, H. Gruppelaar, and J.M. Akkermans, Phys. Rev. C **28**, 587 (1983).
[3] A. Iwamoto and K. Harada, Nucl. Phys. **A419**, 472 (1984).
[4] M. Blann, W. Scobel, and E. Plechaty, Phys. Rev. C **30**, 1493 (1984).
[5] P. Madler and R. Reif, Nucl. Phys. **A337**, 445 (1980).
[6] M.B. Chadwick and P. Obložinský, Phys. Rev. C **44**, R1740 (1991)
[7] M.B. Chadwick and P. Obložinský, Phys. Rev. C **46**, 2028 (1992)
[8] E. Gadioli and P.E. Hodgson, *Pre-equilibrium Nuclear Reactions* (Clarendon Press, Oxford, 1992).
[9] H. Feshbach, Phys. Rev. C **48**, R2553 (1993).
[10] K. Kikuchi and M. Kawai, *Nuclear Matter and Nuclear Reactions* (North-Holland, Amsterdam, 1968), p. 44; M.L. Goldberger, Phys. Rev. **74**, 1269 (1948).
[11] C. Kalbach, Phys. Rev. C **37**, 2350 (1988).
[12] F.C. Williams, Nucl. Phys. **A166**, 231 (1971); E. Betak and J. Dobes, Z. Phys. **A 279**, 319 (1976).
[13] G. Reffo and M. Herman, Nuovo Cimento Lett. **34**, 261 (1982).
[14] K. Sato, Phys. Rev. C **32**, 647 (1985).
[15] P.G. Young, E.D. Arthur, and M.B. Chadwick, Los Alamos National Laboratory Report No. LA-12343-MS (1992).
[16] A. Galonsky, R.R. Doering, D.M. Patterson, and H.W. Bertini, Phys. Rev. C **14**, 748 (1976).
[17] A.A. Cowley, A. van Kent, J.J. Lawrie, S.V. Fortsch, D.M. Whittal, J.V. Pilcher, F.D. Smit, W.A. Richter, R. Lindsay, I.J. van Heerden, R. Bonetti, and P.E. Hodgson, Phys. Rev. C **43**, 678 (1991).
[18] A. Marcinkowski, R.W. Finlay, G. Randers-Pehrson, C.E. Brient, R. Kurup, S. Mellema, A. Meigooni, and R. Taylor, Nucl. Sci. Eng. **83**, 13 (1983).